ISSN 1063-7761, Journal of Experimental and Theoretical Physics, 2022, Vol. 134, No. 4, pp. 449–458. © Pleiades Publishing, Inc., 2022.
Russian Text © The Author(s), 2022, published in Zhurnal Eksperimental'noi i Teoreticheskoi Fiziki, 2022, Vol. 161, No. 4, pp. 533–543.

This article was written for the special issue of JETP dedicated to the centenary of A.E. Chudakov

Analysis of Cosmogenic Neutron Characteristics and the Pulses Counting Rate Using ASD, LSD, and LVD Scintillation Detectors

N. Yu. Agafonova[a,*], M. Aglietta[b,c], P. Antonioli[d], V. V. Ashikhmin[a], G. Bari[d], G. Bruno[e,f], E. A. Dobrynina[a], R. I. Enikeev[a], W. Fulgione[c,e], P. Galeotti[b,c], M. Garbini[d,g], P. L. Ghia[h], P. Giusti[d], E. Kemp[i], A. S. Malgin[a†], A. Molinario[e,j], R. Persiani[d], I. A. Pless[k], O. G. Ryazhskaya[a†], G. Sartorelli[d], I. R. Shakiryanova[a], M. Selvi[d], G. C. Trinchero[b,c], C. F. Vigorito[b], V. F. Yakushev[a], and A. Zichichi[d,g]

[a] *Institute for Nuclear Research, Russian Academy of Sciences, Moscow, 117312 Russia*
[b] *University of Torino and INFN-Torino, Turin, 10125 Italy*
[c] *INAF, Osservatorio Astrofisico di Torino, Turin, 10025 Italy*
[d] *University of Bologna and INFN-Bologna, Bologna, 40127 Italy*
[e] *INFN, Laboratori Nazionali del Gran Sasso, Assergi, L'Aquila, 67100 Italy*
[f] *New York University, Abu Dhabi, 129188 United Arab Emirates*
[g] *Centro Enrico Fermi, Roma, 00184 Italy*
[h] *Laboratoire de Physique des 2 Infinis Irène Joliot Curie, CNRS, Orsay, 91406 France*
[i] *University of Campinas, Campinas, 13083 Brazil*
[j] *Gran Sasso Science Institute, L'Aquila, 67100 Italy*
[k] *Massachusetts Institute of Technology, Cambridge, 02139 USA*
**e-mail: agafonova@inr.ru*

Received October 6, 2021; revised October 30, 2021; accepted October 30, 2021

Abstract—Experimental data obtained using three scintillation detectors are analyzed. The characteristics of cosmogenic neutrons in underground experiments their analytic dependences are considered. The behavior of background counting rate for the LVD detector for two measuring thresholds (0.5 and 5 MeV) are discussed.

DOI: 10.1134/S1063776122040124

1. INTRODUCTION

Cosmogenic neutrons form the main background in underground experiments aimed at the search for rare interactions. First targeted investigations of neutrons were performed with the Artemovsk scintillation detector in 1970s. The energy spectra of neutrons, their underground flux, temporal variation of neutrons, and the neutron yield from muons have been obtained by developing the technique of neutron detection on the LSD and LVD scintillation detectors designed based on the Russian–Italian collaboration.

1.1. Liquid Scintillator

The principle of detection of particles by the scintillation method includes the excitation of molecules, which is converted into the electromagnetic radiation in the visible and ultraviolet ranges with isotropic emission of photons. The basis of a liquid scintillator (LS) is the carbon-containing substance (white spirit [1]), which by weight contains 65 wt % C_kH_{2k+2} paraffins, 15 wt % C_kH_{2k} naphthenes, and 20 wt % aromatic hydrocarbons [2].

The development of white spirit-based LS for large-scale neutrino detectors in the USSR was started in 1965–1968 [1, 3]. This scintillator was later used in experiment at Baksan (BUST), Artemovsk, and in Italy (LSD, LVD).

The general formula of white spirit is C_kH_{2k}, $\bar{k} = 9.6$; the density at a temperature of 20°C is $\rho = 0.778 \pm 0.02$ g/cm^3, the volume expansion coefficient is $(1.23 \pm 0.04) \times 10^{-3}$ deg^{-1}, and the refractive index is 1.5 for light with a wavelength of 420 nm. The burst temperature of white spirit in an open volume is 36 ± 2°C, and its permittivity is $\varepsilon = 2.1$ (twice as high as that

† Deceased.

for dry air). For obtaining the high transparency of the scintillator, the base was purified by the circulation through Al_2O_3 sorbents and zeolite under pressure. The transparency was monitored at a spectrophotometer wavelength of 420 nm by the "leaving the beam" method from the intensity of light passing through a 60-cm liquid column. Shifter POPOP (0.03 g/l) and activator PPO (1 g/l) were diluted in the base. The specific light yield of the LS was 1 photon for 160 eV or 6.25 photon/keV. The LS radiation spectrum and the spectral sensitivity of the photoelectric cathode PMT are in good agreement. The LS in the counter is purged with argon for displacing atmospheric oxygen diluted in the LS and suppressing scintillations. Almost entire amount of oxygen in large volumes of the scintillator is removed by passing through the LS of argon with a volume six time larger than the LS volume. The specific light yield increases thereby approximately twofold [1]. The average transparency after the purification was about 20 m; over this length, the light intensity decreases by e times.

The 1.5-m^3 liquid scintillation counter was constructed in 1979 for long-term large-scale experiments for the search for neutrino radiation bursts from collapsing stellar cores. Seventy-two such counters were used for designing the LSD detector operating from 1984 to 1999 [4]. The LVD facility contains 840 counters [5].

The size of the counter is $1 \times 1 \times 1.5$ m^3; three PMTs with a photocathode diameter of 150 mm are located on its upper face. The counter container was welded from stainless steel sheets of thickness 4 mm. The total mass of the container in assembly was 290 kg (without PMTs and boxes). The light-collecting system consists of a mylar (aluminated) film coating the area of the inner surface of the counter (8×10^4 cm^2) with specular reflection coefficient $\alpha = 0.80$–0.90 and a high-transparency LS (15–25 m) with an optical density of 1.49 for light with $\lambda \approx 420$ nm. In this counter, the method of full collection of light as a result of multiple reflections is used with low losses of light in the course of light collection (absorption in collecting system elements) and a small ratio of the photocathode area to the area of the inner surface of the counter [6]. All counter materials are chemically inert relative to the LS material, which prevents the decrease in its transparency. The scintillator counter mass is 1170 ± 20 kg.

1.2. Underground Neutrons

Because of the high penetrability of neutrons and a quite large nuclear reaction cross section, neutrons are the main hardly eliminated background in underground laboratories. Neutrons can initiate events imitating the sought ones in a wide energy range from tens of kiloelectronvolts to hundreds of megaelectronvolts due to elastic collisions with free protons (in detectors operating with an organic scintillator) or with nuclei of the target material, as well as inelastic collisions with nuclei. Since neutrons are emitted from nuclei and most probably end their free state in a nuclear capture, the emergence of each neutron is associated (apart from its own interactions with matter) with the formation of at least two isotopes (the residual nucleus of the detector or the protector material and of the nucleus that has captured a neutron). The emerging unstable isotopes can initiate a background event by emitting an electron or a gamma quantum. The flux of neutrons emerging from the rock in underground laboratories include neutrons with natural radioactivity as well as cosmogenic neutrons (generated by muons). At depths exceeding 2 km w.e., the cosmogenic neutron flux is 2.5–3 orders of magnitude smaller than the flux of neutrons with the radioactivity of the rock, which are formed in the (α, n) reactions (α particles are emitted by nuclei from the uranium or thorium family, which are contained in the rock) and during spontaneous fission of ^{238}U. The energy of these neutrons does not exceed 30 MeV; their role in producing the background can be eliminated by introducing a protector with a sufficient thickness. However, due to high energy (up to ~1 GeV), cosmogenic neutrons are characterized by large free paths, and the corresponding increase in the thickness of the protector and, hence, its mass increases the probability of formation of neutrons in it. Therefore, the protector itself becomes the source of the neutron background.

In detectors operating on an organic scintillator (LVD, Borexino, KamLAND, BUST, and ASD experiments), which are used in the search for the neutrino flux from the gravitational collapse of a stellar core accompanied by a burst of a second-type supernova, the main reaction is the interaction of an electron antineutrino with a proton, viz., $\bar{\nu}_e p \to n e^+$ is the Raynes–Cowen or inverse beta decay (IBD) reaction. The Raynes–Cowen reaction is characterized by a well identifiable signature and a large cross section; as a result of this reaction, there appears a pair of time-conjugate pulses (e^+ and a 2.2-MeV γ quantum from the np capture).

Cosmogenic neutrons with a high energy (exceeding 10 MeV) can exactly reproduce the IBD signature. Neutrons imitate the reaction signature by producing the first pulse via np scattering (recoil proton ionization loss) and the second pulse via the np capture of a thermalized neutron (the energy of the emitted γ quantum is 2.2 MeV).

2. DETECTION OF NEUTRONS

Neutrons are registered in a scintillation detector by detecting [gamma] quanta with energy higher than the lower threshold ($E > 0.5$ MeV), which is opened in a 1-ms time window behind the trigger ($E > 5$ MeV), which is caused by the passage of a muon or another

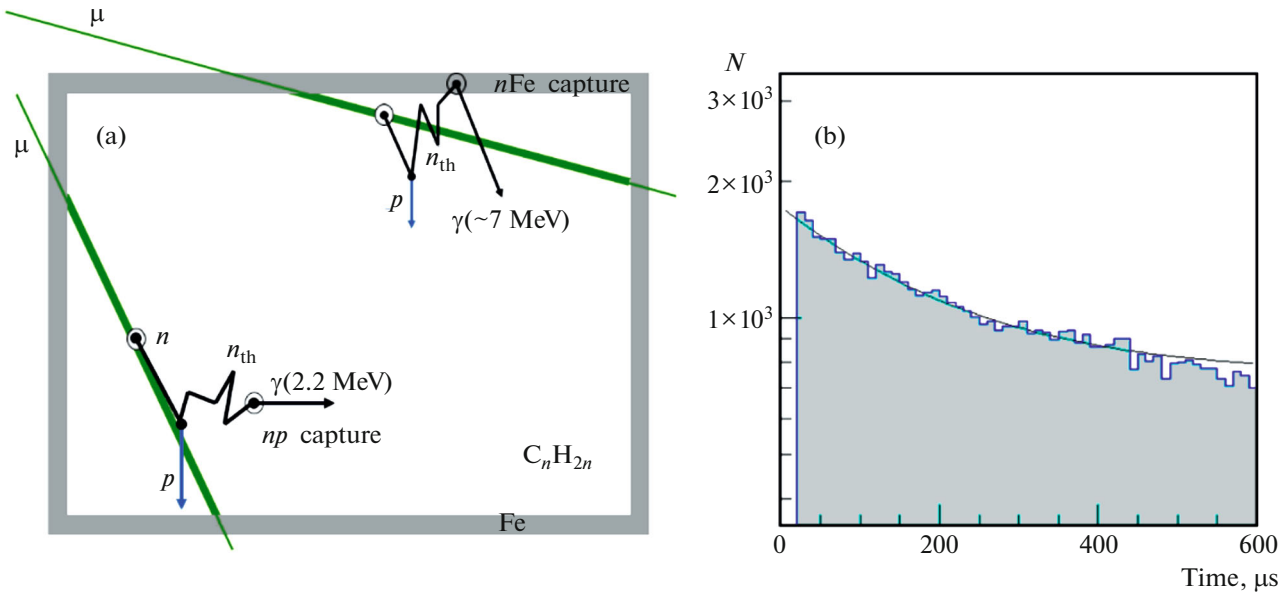

Fig. 1. (a) Diagram of passage of a muon through the counter with generation of neutrons and detection of γ quanta. (b) Time distribution of the number of detected γ quanta with the background; curve is approximation of form $dN_n/dt = B + N_0\exp(-t/\tau)$.

high-energy particle (proton, background γ quantum, and so on).

A muon passing through the setup either generates neutrons by its field (direct-generation neutrons) or generates an electromagnetic or hadron shower, in which secondary neutron are generated. All these neutrons are decelerated in the detector material to approximately 0.4 eV in collisions mainly with protons. Then neutrons are thermalized to energy of 0.025 eV and are captured by the proton of hydrogen ($np \to D^* \to D + \gamma$) or by the Fe nucleus ($n^{56}\text{Fe} \to {}^{57}\text{Fe}^* \to {}^{57}\text{Fe}\,(k\gamma)$, 91.7%; $n^{54}\text{Fe} \to {}^{55}\text{Fe}^* \to {}^{55}\text{Fe}\,(\gamma)$, 5.8%) with the emission of γ quanta with energy of 2.23 MeV or about 8 MeV, respectively (Fig. 1a).

The average lifetime (diffusion time) of a thermalized neutron in a medium can be determined using expression

$$\tau_{\text{diff}} = \frac{1}{v_{\text{th}}\Sigma_a} = 2.05\times10^{-4}\ \text{s},$$

where $v_{\text{th}} = 2198$ m/s is the velocity of a thermalized (0.025 eV) neutron; $\Sigma_a = 0.0222$ cm^{-1} is the macroscopic cross section of the neutron absorption by nuclei of the medium, which is averaged over the Maxwellian neutron spectrum and depends on the chemical formula of the LS (C_kH_{2k}) and density $\rho = 0.78$ g/cm^3.

The separation of γ quanta from the neutron captures and background events is carried out using characteristic exponent $\exp(-t/\tau)$, where τ is the capture time, and the 2D time distribution of background pulses (Fig. 1b). Therefore, the time distribution being registered is the sum:

$$\frac{dN_n}{dt} = B + N_0\exp\left(-\frac{t}{\tau}\right).$$

With account for the detector size and edge effects, $\tau \approx 185$ μs for the scintillator and $\tau \approx 135$ μs for γ quanta from neutron captures at iron.

The efficiency of detection of neutrons distributed isotropically over the counter volume during captures in the scintillator by one counter is $\eta_n = (55 \pm 2)\%$ [7]. This value can be explained by the emission of γ quanta and (to a lesser extent) neutrons from the counter. In the chosen measuring conditions, when a neutron is detected by several counters, efficiency η_n increases to approximately 77%. Gamma quanta with energies from 4 to ~10 MeV (maximal energy of a γ quantum from *n*Fe capture) are registered with efficiency 62% [7]. The high detection efficiency is due to the geometry and large sizes of the detecting volume.

2.1. Artemovsk Experiments

At the beginning of 1970s, at the Artemovsk Scientific Station (ASS), Institute for Nuclear Research, USSR Academy of Sciences (near Artemovsk, now Bakhmut, Ukraine), a experiment for studying neutrons at various depths was constructed; it was also used for analyzing the behavior of the muon nuclear interaction cross section depending on the transferred energy. The ASS setup consisted of three levels of scintillation counters [8]. The upper and lower levels detected charged particles ($0.35 \times 1.4 \times 1.4$ m^3); the middle level contained a counter ($0.7 \times 0.7 \times 0.7$ m^3)

Table 1. Measurements of neutron yield at Artemovsk, LSD, and LVD. Yields are given in the units of $\times 10^{-4} n/\mu/(g/cm^2)$. Values for Y_{LS} (*) have been corrected (see [16])

Experiment	$\bar{E}_\mu$, GeV	H, m w.e.	Y_{LS}, $A = 10.4$	Y_{Fe}, $A = 56$
ASS	16.7 ± 8.2	25	0.36 ± 0.05*	
ASS	86 ± 18	316	0.93 ± 0.12*	
ASD	125 ± 22	570	1.57 ± 0.24*	
LVD	280 ± 18	3300	3.3 ± 0.5	16.4 ± 2.3
LSD	385 ± 39	5200	4.1 ± 0.6*	20.3 ± 2.6

sensitive to both charged particles and neutrons owing to a gadolinium salt dissolved in the scintillator. The detector was triggered when a muon passed through it, and during 200 μs after this event, a burst corresponding to energy yield of γ quanta (delayed pulses) emitted after the capture of a neutron by the gadolinium nucleus was detected or large energy release associated with the passage of a shower through the detector was observed in any level of counters. The experiment was performed at two depths under the ground (at a depth of 316 m w.e. in the salt-mine and at a depth of 25 m w.e. in the plaster-mine.

The Artemovsk scintillation detector (ASD) commissioned in 1978 has a 100-t LS in a cylindrical carcase with approximately equal height and diameter (about 5.5 m). The detector is in the salt-mine at a depth of 570 m w.e. [9]. The energy range was determined by potentialities of electronic devices aimed at detection of the IBD reaction. Muons with a mean energy of 125 GeV generated neutrons in the scintillator of the detector and partly in salt surrounding the setup. The number of neutrons was determined from the time distribution of retarded γ quanta with energy from 0.5 MeV to 10 MeV in the 200-μs time window [10]. The neutron energy required for obtaining the spectrum was determined from the recoil proton energy yield in the elastic *np* scattering reaction with account for quenching in the LS and particles from the *n*C interaction [11].

2.2. LSD and LVD Experiments

The LSD experiment [4] was carried out from 1985 to 1998 in a chamber near the Mont Blanc tunnel (Italy) at a depth of 5200 m w.e. The LVD experiment [5] located under the peak of Gran Sasso mountain range (LNGS, Italy) at depth $\bar{H}$ = 3300 m w.e., H_{min} = 3100 m w.e., provides information since 1991.

The detectors have similar structures — both of them are designed based on a 1.5-m^3 scintillation counter ($1 \times 1 \times 1.5$ m^3). The energy resolution of the counter for energy yield exceeding 20 MeV is about 20%; the range of energy yields being measured is 0.5–500 MeV. The time resolution is 1 μs [6]. The masses of the scintillators and steel parts of the setups are approximately identical (LSD contains 90 t of LS and 100 t of Fe; LVD has 970 t of LS and 1000 t of Fe). Seventy-two counters for LSD form three levels and 3 columns. The LVD contains 840 counters grouped in 3 towers (T1, T2, and T3), each of which forms 7 levels and 5 columns.

Neutron yield at LSD and LVD was determined in different conditions of neutron detection: (i) by the inner counter of the setup, through which a muon had passed (LSD [12]); (ii) by all counters in the inner volume of the setup crossed by a muon (LVD [13]), and (iii) by inner counters with trigger pulses, including the muon counter (LVD [14]). Here, the muon is treated as a single muon as well as a group of muons with accompanying shower or without it.

3. EXPERIMENTAL RESULTS

3.1. Neutron Yield

At the Artemovsk LSD and LVD setups, neutrons generated by muons in the detector material (in the scintillator for ASS [10], ASD [15] and in the scintillator and steel in the structure of counters in LSD [12, 16] and LVD [13, 14, 16]) were measured. Table 1 contains the results of measurements of the neutron yield. The neutron yield from iron was obtained for the LSD and LVD using the calculation of the mass fractions of materials [16] and the detection efficiency for neutrons generated in iron and in the scintillator [7].

The generation of neutrons by the muons flux (neutron yield) with energies exceeding tens of gigaelectronvolts is characterized by muon energy $\bar{E}_\mu$: $Y_n \propto \bar{E}_\mu^\alpha$, where $\alpha = 0.75$–0.80. Comparisons of the values of energy $\bar{E}_\mu$ and depth H in different experiments (see Table 1) shows that energy $\bar{E}_\mu$ is determined with a large error. The calculation of $\bar{E}_\mu$ at the given depth requires the determination of the muon spectrum on the surface, the surface relief, the composition and density of the rock under the detector, as well as the muon energy loss in the material.

The dependences of the neutron yield on muon energy E_μ and atomic number A of the substance were usually described by simple expressions $Y_n(\bar{E}_\mu) = c_A E_\mu^\alpha$ and $Y_n(A) = c_E A^\beta$. As a result of best approximation of experimental data for Y_n, the Malgin universal formula (UF) was derived:

$$Y_n = b_n \bar{E}_\mu^\alpha A^\beta, \quad (1)$$

where $b_n = 4.4 \times 10^{-7}$ $(g/cm^2)^{-1}$, $\alpha = 0.78$, and $\beta = 0.95$ [17, 18]. Being an empirical expression for the main dependence of the yield on E_μ and A, UF connects energy loss b_n of muons in substance A, which

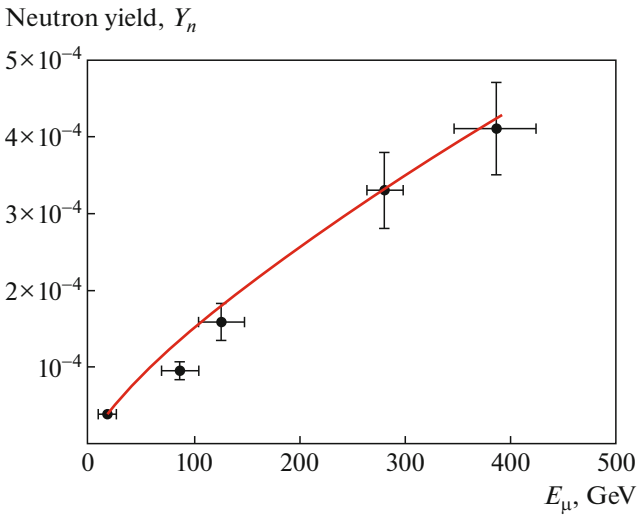

Fig. 2. Measured neuron yields in the scintillator as a function of the mean muon energy. Curve is function $Y_n = 1.4 \times 10^{-7} \times 10.4^{0.95} \bar{E}^{0.78}$.

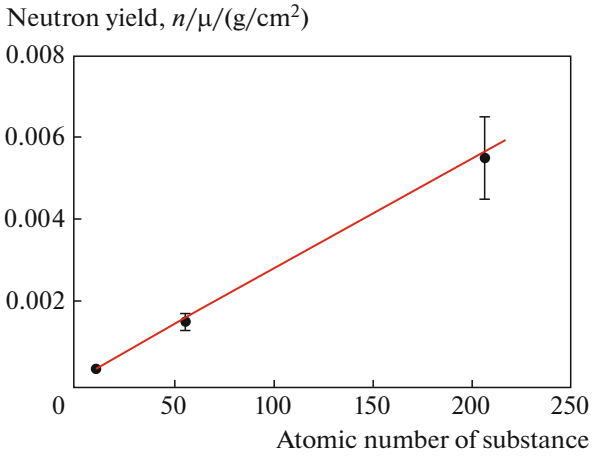

Fig. 3. Measurements of the neutron yield in LS, Fe, and Pb for $\bar{E}_\mu = 280$ GeV; curve is the calculation based on UF.

can generate neutrons under the action of energy $b_n \bar{E}_\mu^\alpha$ and reveals the meaning of coefficients c_A and c_E in dependences $Y_n(\bar{E}_\mu)$ and $Y_n(A)$. In conformity with the results of measurements, UF takes into account the effect of the actual spectrum of the muon flux with energy $\bar{E}_\mu$ on the neutron yield.

As shown in [18], the yield of cosmogenic neutrons is determined by the nuclear and electromagnetic energy losses of muons with ultrarelativistic energies and the nuclear properties of the substance.

Figure 2 shows the values of the neutron yield in the scintillator, which was measured in the ASD, LSD, and LVD experiments, and the $Y_n(\bar{E}_\mu)$ dependence obtained using UF. The universal formula makes it possible to calculate the value of yield Y_n for any substance at any depth of the experiment; in this sense, formula (1) is universal. The UF accuracy is not worse than 20%.

The validity of this formula was confirmed in recent LVD experiments. The LVD structure was supplemented with additional substances: for measuring the neutron yield in iron (Y_n^{Fe}), a 4-cm layer with a total mass of 470 kg was used; for measuring in lead (Y_n^{Pb}), a layer of mass 510 kg (3 cm) was used. For analysis, muons that have passed through two LVD counters and the additional substance (iron or lead) between them were chose were selected. The neutron yields were measured from the difference of the specific numbers of neutrons from muons before and after the introduction of the additional material. With account for the mean free paths of a muon (35.6 g/cm^2 in additional iron and 38.7 g/cm^2 in lead) and the efficiencies in neutron detection (24.4% and 28.0%), the following values of generation of neutrons by muons were obtained $Y_n^{Fe} = (15 \pm 2) \times 10^{-4} n/\mu/(g/cm^2)$ in iron and $Y_n^{Pb} = (55 \pm 10) \times 10^{-4} n/\mu/(g/cm^2)$ in lead). The UF-based calculation gives $Y_n^{Fe}(UF) = 16.3 \times 10^{-4} n/\mu/(g/cm^2)$ and $Y_n^{Pb}(UF) = 56.5 \times 10^{-4} n/\mu/(g/cm^2)$ (see Fig. 3). Yield Y_n^{Pb} was obtained for statistics base of 4 years of analysis (2015–2019). The error of measurement is systematic (larger than statistical error) and is associated with a quite thin lead layer (3 cm), which is insufficient for full development of shower. Large fluctuations of distribution $dN_n/dt = B + N_0 \exp(-t/\tau)$ complicate the determination of number of neutrons $N_0\tau$.

3.2. Energy Spectrum

An important characteristic of cosmogenic neutrons is the generation energy spectrum ($F^s(T)$). This spectrum determines the spectrum of isolated neutrons ($F^{is}(T)$), the neutron penetrability, and effects associated with interaction of neutrons in materials of detectors.

In the LVD experiment, the energy of spectrum of neutrons with energies from 30 to 450 MeV [19], which have been generated by muons in the detector material, were obtained. Muons with mean energy of 280 GeV passed through a detector column, and the detecting volume formed by 60 counters was 72 t of LS. The neutron spectrum was reconstructed using the total neutron yield spectrum in the counters. The correspondence between the energy yield being detected and the neutron energy was established by Monte Carlo calculations. In the energy range from 30 to 120 MeV, points are described by dependence

$F^s(T) \propto T^{-1.11 \pm 0.30}$, while in the energy range from 120 MeV to 450 MeV, it is described by dependence $F^s(T) \propto T^{-2.05 \pm 0.14}$. The shape of the spectrum changes at an energy of about 120 MeV.

In the ASD experiment, the neutron energy spectrum was measured in the range from 20 to 90 MeV [9]. Neutrons were generated in salt by a muon flux with a mean energy of 125 GeV. The neutron energy was determined from the energy yield of recoil protons in the elastic scattering reaction with account for quenching in LS. The spectrum exponent was determined to within 20% ($F^{is}(T) \propto T^{-0.5 \pm 0.1}$).

The experimental data obtained on ASD and LVD led to the conclusion [18] that the cosmogenic neutron energy ranges from zero to ~1 GeV. The cosmogenic neutron generation spectrum $F^s(T)$ has the three-component structure. In the first component, evaporation neutrons with the Maxwellian spectrum and a maximal energy of about 30 MeV dominate. Neutrons of this component constitute approximately 75% of the total number of cosmogenic neutrons. Neutrons with energy from 30 to 1000 MeV form the second and third spectral components. The form of these components T^{-1} and T^{-2} with inflection at energy $T_{cr} \approx 60(A^{0.25} - 0.67)$ MeV follows from the additive quark model of deep inelastic soft processes with inclusion of the effects of passage of neutrons through the nucleus [18, 20]. Spectrum $F^{is}(T)$ of isolated cosmogenic neutrons emerging from the ground also includes three components and is limited by energy of about 1 GeV. The first component also has the form of the Maxwellian distribution with a limiting energy of 30 MeV. The main factor determining the shape of the second and third components of spectrum $F^{is}(T)$ is the size of the region from which cosmogenic neutrons reach the detector. Under the action of this factor, the second component takes form $F^{is}(T) \propto T^{-0.6}$, while the third component is transformed into $F^{is}(T) \propto T^{-2.6}$ [18, 20].

3.3. Neutron Flux

As shown in [21], cosmogenic neutron flux $F_n(H)$ can be expressed in terms of rate $R_n(H)$ of formation of neutrons at the chamber–rock interface at depth H and chamber surface area S_c:

$$F_n(H) = R_n(H)/S_c.$$

The rate of neutron formation in rock volume V is determined by effective thickness l_n of the layer and density ρ of the rock surrounding the chamber, from which neutrons pass to the chamber, and depends on the global muon intensity $I_\mu(H)$ and neutron yield $Y_n(H)$:

$$R_n(H) = I_\mu(H)V\rho Y_n(H)\ [n\ s^{-1}].$$

Substituting the expression for $R_n(H)$ and $V \approx S_c l_n$, we obtain the following expression for the flux:

$$F_n(H) = I_\mu(H)Y_n(H)l_n\rho\ [n\ cm^{-2}\ s^{-1}], \quad (2)$$

which is the cosmogenic neutron flux in the ground at depth H.

Product $l_n\rho$ [g/cm^2] is attenuation length λ_n characterizing suppression k of the isotropic neutron flux in the ground ($k = \exp(-L/\lambda_n)$, L [g/cm^2] being the thickness of the rock layer). We will use the relation between $\bar{E}_\mu$ and H in form

$$\bar{E}_\mu = [1 - \exp(-bH)]\frac{\varepsilon_\mu}{\gamma_\mu - 2},$$

where $\varepsilon_\mu = 693$ GeV, $\gamma_\mu = 3.77$, and $b = 0.4$ (km w.e.)$^{-1}$ for the standard rock and a flat surface [22]. Substituting the value of $\lambda_n = 35$ g/cm^2 into the expression for $F_n(H)$ and writing yield $Y_n(H)$ in form (1) for $A = 22$, we obtain the neutron flux emerging from the ground through the chamber–standard rock interface [21]:

$$F_n(H) = 2.9\times10^{-4} I_\mu(H)\bar{E}_\mu^{0.78}(H)\ [n\ cm^{-2}\ s^{-1}]. \quad (3)$$

For muon intensity I_μ, we can use expression

$$I_\mu(H) = 68\times10^{-6}\exp\left(-\frac{H}{0.285}\right) + 2.1\times10^{-6}\exp\left(-\frac{H}{0.698}\right)$$

from [23]. Dependence $F_n(H)$ of the flux, which is calculated using formula (3) is shown in Fig. 4. With the help of the Monte Carlo simulation using GEANT4 platform, the neutron flux in the rock of the underground hall of the LVD detector was calculated: $F_n^{MC} = 4.58 \times 10^{-10}$ cm^{-2} s^{-1} [24].

3.4. Time Variation of Neutron Flux

In the LVD experiment, it was found [25, 26] that cosmogenic neutron flux F_n^0 experiences seasonal variations under the action of two factors: (i) variation $\delta I_\mu/I_\mu$ of the muon intensity [27] and (ii) variation $\delta N_n/N_n$ of the specific number of neutrons. At the depth of the LVD, the neutron flux variations have amplitude

$$1 + \frac{\delta F_n}{F_n^0} = \left(1 + \frac{\delta I_\mu}{I_\mu}\right)\left(1 + \frac{\delta N_n}{N_n}\right) = 1.015\times1.077;$$

i.e., $\delta F_n/F_n^0(I_\mu, N_n) = 9.3\%$.

The main source of seasonal variations of the neutron flux under the ground are variations $\delta\bar{E}_\mu$ of the mean muon energy [28] under the assumption that variations $\delta N_n/N_n$ depend only on $\bar{E}_\mu$. The amplitude of variations of the number of neutrons associated with $\delta\bar{E}_\mu$ is five times larger than the amplitude of variations δI_μ. As follows from analysis of the mechanism of temperature variations of muon flux characteristics [18, 29], this is explained by a stronger (as compared to I_μ) dependence of energy $\bar{E}_\mu$ on the temperature effect. Assuming that $\delta F_n/F_n^0 = 9.3\%$, we obtain the following expression for seasonal modulations of the flux of neutrons formed in substance A at the LVD depth:

$$F_n(t, A) = F_n^0(H, A)[1 + 0.093\cos(2\pi(t - t_n^0)/T_m)].$$

The detection of stronger modulations of the cosmogenic neutron flux as compared to the muon flux provokes the wish to connect with them the signal modulation in the DAMA/LIBRA experiment of about 7% [30]. This contradicts the difference in modulation phases of the neutron flux, which have been determined from the LVD data ($t_n^0 = 185 \pm 18$ days) and of the DAMA/LIBRA signal ($t_{D/L}^0 = 152.5$ days). Nevertheless, with account for the large indeterminacy of phase t_n^0, which is associated to a considerable extent with irregular temperature oscillations, the influence of neutron flux modulations on the DAMA/LIBRA signal cannot be ignored as yet [8].

4. NEUTRONS AND GAMMA QUANTA FROM THE CHAINS OF URANIUM AND THORIUM DECAY

The background in the LSD and LVD detectors is determined by nuclear decays of uranium ^{238}U, thorium ^{232}Th, and potassium ^{40}K, as well as neutrons in the (α,n) reactions on rock elements from the α particles generated from daughter and α-active nuclei of these series following radon and secondary neutrons formed during interactions of muons. This background was studied not only within the problem of determining the background for the neutrino experiment, but also for determining correlations associated with atmospheric meteorological effects, gravitational effects of the relative motion of the Earth and the Moon, and tectonic activity.

The background of single pulses in LVD with energy $E > 5$ MeV is caused by neutrons from the interaction of muons in the rock around the detector, as well as radioactivity of rock and of the setup material. Figure 5 shows the background detected by triggers for towers T1, T2, and T3. It can be seen that the middle tower is characterized by the lowest value (red curve). The mean counting rate is 4.6×10^{-4} pulse/s/counter for T1, 3.4×10^{-4} pulse/s/counter for T2, and 7.4×10^{-4} pulse/s/counter for T3. First tower T1 is surrounded by rock from three sides, while second tower T2 is surrounded by rock from two short sides. The counting rate for T3 is larger than the other two rates because the third counter is surrounded by rock from two sides and is open to the laboratory hall space at one of long sides. Background particles are collected from the large area of the hall and get into the detector.

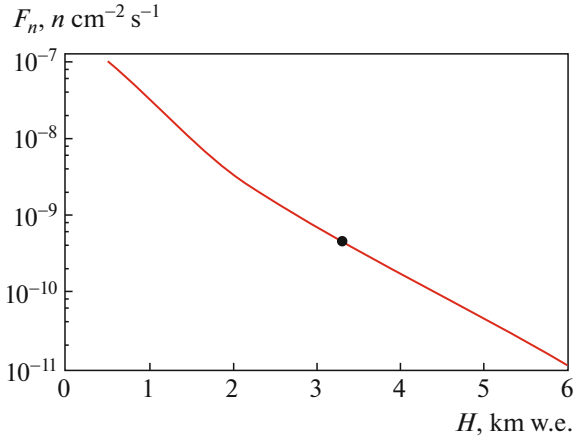

Fig. 4. Total neutron flux from muons in rock as a function of depth. Curve is the UF-based calculation (standard rock $A = 22$) [21]. Bullet is the Monte Carlo calculation for the rock of the Gran Sasso underground laboratory for 3300 m w.e.

The counting rate of the detector with energy $E > 0.5$ MeV is represented in Fig. 6 (upper curve, right axis). These are γ-quanta pulses from the decays of daughter nuclei of radon ^{222}Ra with a half-life of 3.8 days. Gamma radiation is mainly produced by the ^{214}Bi nuclei, which are transformed due to β decay into ^{214}Po with characteristic time $\tau = 19.7$ min. The γ-radiation energy spectrum embraces the range from 0.6 to 2.5 MeV. The lower two curves show the count rates of single triggers ($E > 5$ MeV) of the outer and inner counters; the mean values over 4 years of statistics are 1.5×10^{-3} pulse/s/counter and 0.5×10^{-3} pulse/s/counter, respectively.

The spikes in the temporal series of events with $E > 0.5$ MeV are associated with the injection of radon to the hall atmosphere from microcracks in the rock. The radon concentration in the hall is affected by technical activity in experiments [31, 32], seismic activity, and tidal forces. We also detected seasonal variations of natural radioactivity background of the underground premises due to seasonal oscillations of the radon concentration, which are associated with temperature variation of ground water as well as the temperature and humidity of the underground cham-

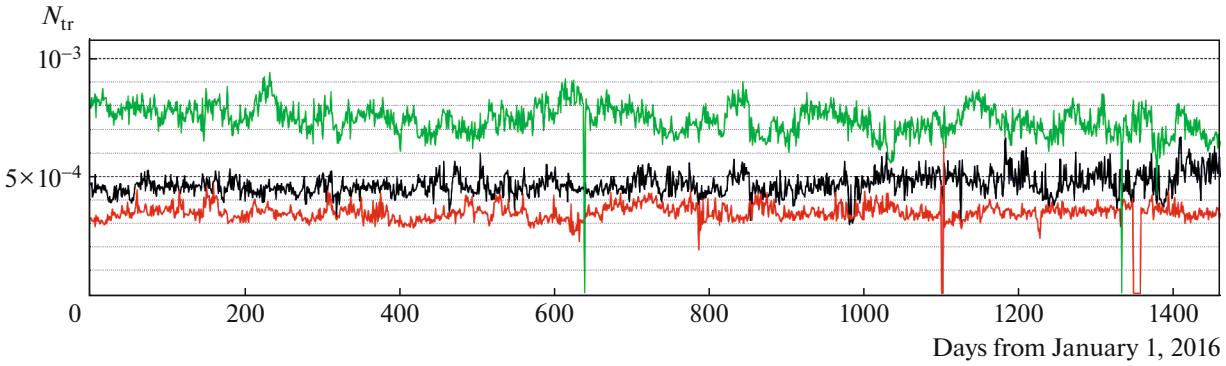

Fig. 5. Time series of the counting rate for single triggers, recalculated per counter per second, for inner counters of T1 (middle black curve), T2 (lower red curve), and T3 (upper green curve). Inner (80) counters are selected identically.

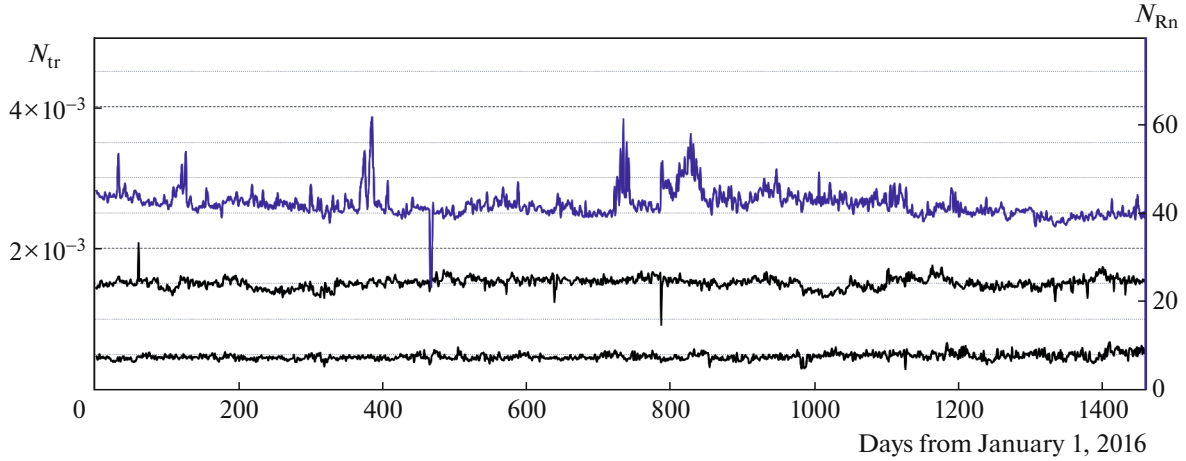

Fig. 6. Time series of the counting rate for single triggers, recalculated per counter per second: upper curve (right axis) represents low-energy pulses; middle curve (left axis) represents single triggers for outer counters; lower curve (left axis) represents single trigger pulses for inner counters.

ber atmosphere. The amplitude of measured variations is $(4 \pm 2)\%$; phase $\phi = 8.1 \pm 0.4$ months [26].

The possibility of studying the radon concentration variations under the ground were noted for the first time after the detection of an anomalous increase of the background counting rate of the LSD during most intense seismic disturbances in Italy (September 1997). Later, an analogous dramatic correlation was found between the increase in the LVD counting rate and intense earthquakes in Turkey (August, November 1999). The effect was observed from two days to several hours prior to earthquakes. The targeted search for correlations between radon spikes in LVD data ($E > 0.5$ MeV) and earthquake precursors is carried out at present [33].

5. CONCLUSIONS

The characteristics of cosmogenic neutrons, which have been measured in experiments at Artemovsk ASD, LSD, and LVD, are the properties of the equilibrium neutron components of hadron accompaniment of muons in a substance.

1. The main quantitative characteristic of neutron is their yield, viz., the quantity determining the properties of the substance to generate neutrons under the action of muons. The main dependence of the neutron yield on the mean energy of the muon flux and the mass number of the substance is described by UF

$$Y_n(\bar{E}_\mu, A) = b_n \bar{E}_\mu^{0.78} A^{0.95}, \quad b_n = 4.4\times10^{-7}\ \text{cm}^2\ \text{g}^{-1}.$$

2. The validity of UF confirms the results of measurements of the neutron yield in the ASD and LSD scintillator, as well as new values of the cosmogenic neutron yield $Y_n^{Fe} = (15 \pm 2) \times 10^{-4} n/\mu/(\text{g/cm}^2)$ from muons in iron and $Y_n^{Pb} = (55 \pm 10) \times 10^{-4} n/\mu/(\text{g/cm}^2)$ in lead, which have been obtained using the LVD detector.

3. Using UF, we have also obtained the dependence of the total flux of neutrons formed by muons in the ground:

$$F_n(H, A) = b_n \lambda_n I_\mu(H) \bar{E}_\mu^{0.78} A^{0.95},$$

the value of which for the depth and rock composition of LNGS is almost equal (to within the errors) to the value calculated by the Monte Carlo method using GEANT4.

4. The dependences for the spectrum of isolated neutrons and the spectrum in the source have been obtained from the energy spectra measured at ASD and LVD.

5. The LVD data were used for determining the seasonal variations of the flux of neutrons generated by muons. Which amount to 9.3%, as well as the seasonal variations of the natural radioactivity background (4%).

The study of the background in the underground laboratory requires a more detailed analysis of data. The LVD detector background has various sources of its variation, such as seasonal variations, lunar–solar tides, and seismic activity. The forms of variations of the count rates for background pulses differ in amplitude and duration. During 30 years of LVD operation, rich statistical data have been accumulated; we believe that this will enable researchers to separate the background components and to single out various effects associated with background variation.

ACKNOWLEDGMENTS

The authors are grateful to the staff of the EMDN Laboratory of the Institute for Nuclear Research, Russian Academy of Sciences, who developed, realized, and contributed to the ASD, LSD, and LVD experiments, the ideas of which are described in this article and who are no more with us.

REFERENCES

1. A. V. Voevodskii, V. L. Dadykin, and O. G. Ryazhskaya, Prib. Tekh. Eksp., No. 1, 85 (1970).
2. S. A. Leont'eva, Zh. Anal. Khim. **32**, 1638 (1977).
3. V. L. Dadykin, Preprint INR No. 1297/2011 (Inst. Nucl. Res. RAS, Moscow, 2011).
4. G. Badino, G. Bologna, C. Castagnoli, W. Fulgione, P. Galeotti, O. Saavedra, V. L. Dadykin, V. B. Korchaguin, P. V. Korchaguin, A. S. Malguin, O. G. Ryazhskaya, A. L. Tziabuk, V. P. Talochkin, G. T. Zatsepin, and V. F. Yakushev, Nuovo Cim. C **7**, 573 (1984).
5. G. Bari, M. Basile, G. Bruni, G. Cara Romeo, A. Castelvetri, L. Cifarelli, A. Contin, C. Del Papa, P. Giusti, G. Iacobucci, G. Maccarrone, T. Massam, R. Nania, V. O'Shea, F. Palmonari, E. Perotto, et al., Nucl. Instrum. Methods Phys. Res., Sect. A **277**, 11 (1989).
6. N. Yu. Agafonova and A. S. Malgin, Opt. Spectrosc. **119**, 712 (2015).
7. N. Yu. Agafonova et al. (LVD Collab.), J. Phys.: Conf. Ser. **409**, 012139 (2013).
8. L. B. Bezrukov, V. I. Beresnev, G. T. Zatsepin, M. I. Nyunin, O. G. Ryazhskaya, and L. I. Stepanets, Sov. J. Nucl. Phys. **15**, 176 (1972).
9. V. I. Beresnev, A. Chudin, R. I. Enikeev, P. V. Korchagin, V. B. Korchagin, A. S. Mal'gin, O. G. Ryazhskaya, V. G. Ryasnyi, V. P. Talochkin, V. F. Yakushev, and G. T. Zatsepin, Prib. Tekh. Eksp., No. 6, 48 (1981).
10. L. B. Bezrukov, V. I. Beresnev, G. T. Zatsepin, O. G. Ryazhskaya, and L. I. Stepanets, Sov. J. Nucl. Phys. **17**, 51 (1973).
11. F. F. Khalchukov et al., in *Proceedings of the 20th International Cosmic Ray Conference ICRC, Moscow* (1987), Vol. 2, p. 266.
12. M. Aglietta et al., Nuovo Cim. C **12**, 467 (1989).
13. N. Yu. Agafonova, V. V. Boyarkin, V. L. Dadykin, E. A. Dobrynina, R. I. Enikeev, A. S. Mal'gin, V. G. Ryasnyi, O. G. Ryazhskaya, I. R. Shakir'yanova, and V. F. Yakushev (LVD Collab.), Bull. Russ. Acad. Sci.: Phys. **75**, 408 (2011).
14. M. Aglietta et al., in *Proceedings of the 26th International Cosmic Ray Conference ICRC, Salt Lake City* (1999), Vol. 2, p. 44; hep-ex/9905047.
15. O. G. Ryazhskaya, Doctoral (Phys. Math.) Dissertation (Inst. Nucl. Res. RAS, Moscow, 1986).
16. N. Yu. Agafonova and A. S. Malgin, Phys. At. Nucl. **76**, 607 (2013).
17. N. Yu. Agafonova and A. S. Malgin, Phys. Rev. D **87**, 113013 (2013).
18. A. S. Malgin, Doctoral (Phys. Math.) Dissertation (Inst. Nucl. Res. RAS, Moscow, 2018).
19. N. Yu. Agafonova, V. V. Boyarkin, V. L. Dadykin, E. A. Dobrynina, R. I. Enikeev, V. V. Kuznetsov, A. S. Malgin, O. G. Ryazhskaya, V. G. Ryasny, V. F. Yakushev, and N. M. Sobolevsky, Bull. Russ. Acad. Sci.: Phys. **73**, 628 (2009).
20. A. S. Malgin, J. Exp. Theor. Phys. **125**, 728 (2017).
21. A. S. Malgin, Phys. At. Nucl. **78**, 835 (2015).
22. D. E. Groom et al., At. Data Nucl. Data Tabl. **78**, 183 (2001).
23. D.-M. Mei and A. Hime, Phys. Rev. D **73**, 053004 (2006).
24. R. Persiani, PhD Thesis (Univ. of Bologna, 2011).
25. N. Yu. Agafonova (on behalf of the LVD Collab.), arXiv:1701.04620; in *Proceedings of the 25th ECRS Conference, 2016*, _eConf C16-09-04.3.
26. N. Yu. Agafonova, V. V. Ashikhmin, V. L. Dadykin, E. A. Dobrynina, R. I. Enikeev, A. S. Malgin, O. G. Ryazhskaya, I. R. Shakiryanova, V. F. Yakushev, and LVD Collab., Bull. Russ. Acad. Sci.: Phys. **81**, 512 (2017).

27. N. Agafonova et al. (LVD Collab.), Phys. Rev. D **100**, 062002 (2019); arXiv: 1909.04579 [astro-ph.HE].
28. A. S. Malgin, J. Exp. Theor. Phys. **121**, 212 (2015).
29. N. Yu. Agafonova and A. S. Malgin, J. Exp. Theor. Phys. **132**, 73 (2021).
30. R. Bernabei, P. Belli, F. Cappella, V. Caracciolo, S. Castellano, et al., Eur. Phys. J. C **73**, 2648 (2013); arXiv: 1308.5109 [astro-ph.GA].
31. N. Yu. Agafonova, V. A. Alekseev, E. A. Dobrynina, et al., Preprint INR No. 1071/2001 (Inst. Nucl. Res. RAS, Moscow (2001).
32. N.Yu. Agafonova, V. V. Ashikhmin, E. A. Dobrynina, R. I. Enikeev, A. S. Mal'gin, K. R. Rudakov, O. G. Ryazhskaya, I. R. Shakir'yanova, V. F. Yakushev, and LVD Collab., Bull. Russ. Acad. Sci.: Phys. **83**, 614 (2019).
33. N. S. Khaerdinov, D. D. Dzhappuev, K. Kh. Kanonidi, A. U. Kudzhaev, A. N. Kurenya, A. S. Lidvansky, V. B. Petkov, and M. N. Khaerdinov, Bull. Russ. Acad. Sci.: Phys. **85**, 1317 (2021).

Translated by N. Wadhwa